



UNIVERSITY OF LEEDS

This is a repository copy of *Understanding the differences in wear testing method standards for total knee replacement*.

White Rose Research Online URL for this paper:

<https://eprints.whiterose.ac.uk/186919/>

Version: Accepted Version

Article:

Abdelgaied, A, Fisher, J and Jennings, LM orcid.org/0000-0003-1446-4511 (2022)
Understanding the differences in wear testing method standards for total knee replacement. *Journal of the Mechanical Behavior of Biomedical Materials*. 105258. ISSN 1751-6161

<https://doi.org/10.1016/j.jmbbm.2022.105258>

© 2022, Elsevier. This manuscript version is made available under the CC-BY-NC-ND 4.0 license <http://creativecommons.org/licenses/by-nc-nd/4.0/>.

Reuse

This article is distributed under the terms of the Creative Commons Attribution-NonCommercial-NoDerivs (CC BY-NC-ND) licence. This licence only allows you to download this work and share it with others as long as you credit the authors, but you can't change the article in any way or use it commercially. More information and the full terms of the licence here: <https://creativecommons.org/licenses/>

Takedown

If you consider content in White Rose Research Online to be in breach of UK law, please notify us by emailing eprints@whiterose.ac.uk including the URL of the record and the reason for the withdrawal request.



eprints@whiterose.ac.uk
<https://eprints.whiterose.ac.uk/>

1
2
3
4
5
6
7
8
9
10
11
12
13
14
15
16
17
18

**Understanding the Differences in Wear Testing Method Standards for
Total Knee Replacement**

A Abdelgaied¹, J Fisher², LM Jennings^{2*}

¹Department of Engineering, Nottingham Trent University, Nottingham, UK

²Institute of Medical & Biological Engineering, School of Mechanical Engineering,
University of Leeds, Leeds, UK

*Corresponding author

Email: l.m.jennings@leeds.ac.uk (LMJ)

19 **Abstract:**

20 Preclinical evaluation of the wear of total knee replacements (TKR) is usually
21 undertaken using International Standards Organization (ISO) test methods. Two
22 international standards for the preclinical wear simulation of TKRs have been
23 developed; using either force or displacement control. In addition, based on
24 previously published measured kinematics of healthy subjects, a gait cycle
25 (displacement control) was also developed at the University of Leeds, which pre-
26 dates the ISO displacement control standard. Furthermore, different test methods
27 have adopted different approaches to defining the centres of rotation and polarity
28 (direction of application) of motions. However, the effects of using these different
29 control regimes and input conditions on the kinematics, contact mechanics, and wear
30 of any one TKR have not been fully investigated previously.

31 The current study investigated the kinematics, contact mechanics, and wear
32 performance of a TKR when running under ISO force and displacement control test
33 methods as well as the Leeds gait cycle inputs using experimental and computational
34 simulation methods, with the aim of understanding the mechanical and tribological
35 outcomes predicted by the different test method standard conditions. Three ISO wear
36 testing standards were investigated using a mid-size Sigma curved TKR (DePuy,
37 UK), with moderately cross-linked UHMWPE curved inserts; ISO-14243-3-2004, ISO-
38 14243-3-2014 and ISO-14243-1-2009. In addition, the Leeds displacement control
39 gait cycle was also investigated.

40 According to the computational simulation predictions, reversing the anterior-posterior
41 (AP) displacement and tibial rotation polarities in the displacement control ISO-2014
42 standard compared to the ISO-2004 standard resulted in high stress, of more than 65
43 MPa, at the posterior edge of the inserts with more than 10% increase in wear rate for
44 this TKR design. Although Leeds gait input kinematics produced femoral rollback, it
45 did not result in high stress edge loading on the posterior lip of the insert. This was
46 attributed to different test input kinematics and different centres of rotation of the
47 femoral component adopted in the displacement control standard ISO-2014 and
48 Leeds gait test methods. The predicted AP displacement and tibial rotation from the
49 force control ISO-2009 had different polarities and magnitudes to the corresponding
50 displacement control profiles. In addition, the predicted wear rate, from the
51 computational model, under the force control ISO-2009 standard was more than
52 double that predicted under displacement control ISO standards due to the increased

53 AP displacement and tibial rotation motions predicted under the force control
54 standard.
55 These major differences, in the mechanics and wear, between different test methods
56 imply that each standard must therefore be used with its own predicate control results
57 from a device with proven clinical history and results across different standards
58 should never be compared, as the choice of test method standard may well be
59 dependent on the design solution for the knee. Clinically, the kinematics in the
60 population are extremely variable, which results in highly variable wear rates. While a
61 standard method is necessary, on its own it is not adequate and needs to be
62 supported by tests under a portfolio of representative conditions with different
63 kinematic conditions, different soft tissue constraints, as well as with different
64 alignments, so that the variability and range of wear rates expected clinically might be
65 determined. This study enables further progress towards the definition of such a
66 portfolio of representative conditions, by deepening the understanding of the
67 relationships between currently used input conditions and the resulting mechanical
68 and wear outputs.

69

70 **Keywords:**

71 Total knee replacements; Preclinical studies; ISO test methods; Experimental
72 simulation; Computational simulation

73 **1. Introduction:**

74 Total knee replacement (TKR) is currently facing a new challenge, due to the
75 increasing number of younger and more active patients requiring TKR (National Joint
76 Registry 2020). The number of TKR primaries recorded in patients under 60 years in
77 England, Wales and Northern Ireland increased by more than 22% between 2013 and
78 2019 (National Joint Registry 2014, National Joint Registry 2020). In addition, the
79 revision rate amongst this patients' group (under 60 years) was more than 10 times
80 that amongst patients over 75 years (National Joint Registry 2020).

81
82 Preclinical evaluation and understanding the long-term wear performance of TKR is
83 therefore important, particularly in these groups. Experimental full-joint simulation has
84 extensively been used for the preclinical evaluation of TKR (Fisher, et al. 2010,
85 Jennings, et al. 2007, Galvin, et al. 2009, Asano, et al. 2007). The advancements in
86 experimental simulators, with improved performance and capabilities, enabled such
87 simulations to be undertaken under more complex and clinically relevant conditions
88 including the influence of activity, materials, and surgical alignment (Abdelgaied,
89 Fisher and Jennings 2017, Johnston, et al. 2018, Johnston, et al. 2019).

90
91 International Standards Organization (ISO) wear testing method standards specify the
92 relative angular movement between articulating components, the pattern of the
93 applied force, speed and duration of testing, sample configuration and test
94 environment to be used for the preclinical wear testing of total knee joint prostheses
95 (ISO-14243-1 2009, ISO-14243-3 2014). Based on an average patient, two different
96 international standards have been developed, such that the anterior-posterior (AP)
97 displacement of the tibial component and tibial rotation can be driven in either force
98 (ISO-14243-1 2009) or displacement control (ISO-14243-3 2004, ISO-14243-3 2014).
99 In the displacement control standard, the AP displacement and tibial rotation that
100 occur during the gait cycle are predefined. In the force control standard, the inputs are
101 AP force and tibial rotation torque profiles, allowing the TKR to move according to the
102 applied forces, with TKR design, alignment of the TKR, and the applied constraints
103 simulating the cruciate ligaments action (Abdelgaied, Fisher and Jennings 2018, ISO-
104 14243-1 2009). Displacement and force control standards should be utilised to
105 answer different research questions. If the aim of the research is to study a specific
106 factor, such as material for example, while eliminating other factors, such as friction

107 and design parameters, using a displacement control method would be more
108 appropriate. In studies where the kinematics are not known or where it is important to
109 consider the effects of other factors such as friction and design, using a force control
110 method may be the better choice (Abdelgaied, Fisher and Jennings 2018, Johnston,
111 et al. 2018, Johnston, et al. 2019). Furthermore, different test methods have adopted
112 different approaches to the femoral centre of rotation, in particular in the sagittal
113 plane, i.e. the flexion-extension axis, and the axis of rotation of the femoral
114 component relative to the machine frame. (ISO-14243-3 2004, ISO-14243-1 2009,
115 ISO-14243-3 2014). In addition, there have been differences in polarity definitions, i.e.
116 direction of application of motions/forces, (referred to as 'sign convention' within the
117 ISO standards). Such differences in centres of rotation and polarity of motions will
118 affect the effective motions at the articulating surfaces, the contact mechanics,
119 kinematics, and hence wear of TKR. In addition, based on measured kinematics of
120 healthy subjects (Lafortune, et al. 1992), and pre dating the first ISO knee wear test
121 methods being developed, a displacement controlled gait profile was developed at the
122 University of Leeds and extensively used to systematically study many factors
123 independently (Barnett, et al. 2001, Jennings, et al. 2007, Galvin, et al. 2009, Fisher,
124 et al. 2010, Abdelgaied, et al. 2011, Abdelgaied, et al. 2014, Abdelgaied, Fisher and
125 Jennings 2018).

126

127 Using a simplified mathematical model to describe the mechanics of the knee joint,
128 Morrison calculated the forces transmitted to the knee joint from gait measurements
129 of healthy male and female volunteers, assuming the normal knee joint to function
130 according to the mechanical principals (Morrison 1970, Paul 1970). It is understood
131 that the calculated knee forces during gait by Morrison and Paul (Morrison 1970, Paul
132 1970, Paul and McGrouther 1975, Paul 1976) formed the basis for the force
133 controlled ISO-14243-1 2002 and ISO-14243-1 2009 standard test protocols for TKR,
134 with the main difference between the two standards being the anterior-posterior
135 motion and tibial rotation restraint systems (ISO-14243-1 2002, ISO-14243-1 2009).
136 These gait force profiles were inputs to early experimental force control knee
137 simulation studies of TKR (Walker, et al. 1997, Sathasivam and Walker 1997,
138 Johnson, Andriacchi and Laurent 2000, Sutton, et al. 2010). It is understood that the
139 measured output AP displacement and tibial rotation from these experimental studies,
140 using the force inputs and a fixed bearing TKR, formed the basis for the displacement

141 controlled ISO-14243-3 2004 and ISO-14243-3 2014 standard test protocols for TKR
142 (ISO-14243-3 2004, ISO-14243-3 2014).

143
144 Both force and displacement control ISO standard wear testing methods adopt a
145 centre of the rotation of the femoral component representing an average centre of the
146 femoral distal and posterior radii. The axial force and flexion-extension angle (of the
147 femoral component) is also the same for ISO force and ISO displacement control
148 methods, with the axial force profile varying between 268 N and 2600 N and the
149 flexion-extension profile varying between 0° and 60°. The AP profiles vary between
150 110 N and -265 N and between 0 mm and 5.2 mm (ISO-14243-3 2014) for the force
151 and displacement protocols respectively. The tibial rotation profiles vary between -1.0
152 Nm and 6.0 Nm and between -1.9° and 5.7° for the force and displacement protocols
153 respectively (ISO-14243-1 2009, ISO-14243-3 2014). The only difference between
154 the displacement control ISO-14243-3 2004 and ISO-14243-3 2014 is reversal of AP
155 displacement and tibial rotation polarities between the two standards, as shown in
156 Table 1 (ISO-14243-3 2004, ISO-14243-3 2014). The reversed polarities in the new
157 ISO-14243-3 2014 are thought to produce more clinically relevant test conditions,
158 such as femoral rollback, which could not be achieved using ISO-14243-3 2004
159 standard (Brockett, et al. 2016).

160
161 The University of Leeds displacement control test method, which pre-dates the ISO
162 displacement control standard, used axial force and flexion-extension profiles similar
163 to those of the ISO test methods. The AP displacement and tibial rotation angle
164 profiles were however, different from those of the ISO test protocols and were based
165 on the data of Lafortune et al., who analysed healthy patients without replacement
166 prostheses (Lafortune, et al. 1992). This resulted in AP displacement and tibial
167 rotation profiles varying between -3.5 mm and 10 mm and between -5.0° and 5.0°
168 respectively (Barnett, et al. 2001, McEwen, et al. 2005, Fisher, et al. 2010) (Table 1).
169 In addition, the Leeds displacement control test method adopted a distal centre of
170 rotation of the femoral component to replicate femoral rollback (Brockett, et al. 2016).

171
172
173
174

175

176

177 Table 1: Different test methods for total knee replacements

	ISO-14243-1 2009	ISO-14243-3 2004	ISO-14243-3 2014	Leeds
Femoral centre of rotation	ISO (an average centre of the femoral distal and posterior radii)			Distal
Control	Force	Displacement		
AP range	268 N to 2600 N	-5.2 mm to 0 mm	0 mm to 5.2 mm	-3.5 mm to 10 mm
Tibial rotation range	-1.0 Nm to 6.0 Nm	-1.9° to 5.7°	-5.7° to 1.9°	-5.0° to 5.0°

178

179 The effects of using these different control regimes and input conditions on the
180 kinematics, contact mechanics, and wear of any one TKR have not been fully
181 investigated. The aim of this study was therefore to investigate the kinematics,
182 contact mechanics and wear of the same TKR design when the ISO force and
183 displacement control standards, and Leeds displacement control methods were
184 followed, using a combination of experimental and computational simulation methods.
185 This would provide understanding of the differences in mechanical and tribological
186 outcomes predicted by the different test methods. In addition, the computationally
187 predicted output kinematics using the ISO force control standard inputs (including the
188 recommended ISO soft tissue constraints) were compared to the measured output
189 kinematics from the experimental simulator to investigate the possibility of using the
190 force control standard to generate displacement control inputs. In this approach,
191 computational models could be used to predict displacements from the TKR
192 responses to the force control standard inputs and soft tissue constraints. The
193 resulting kinematics could then be used as displacement control inputs if required.

194

195 **Materials/Methods:**

196 A combined experimental and computational approach was used to investigate the
197 effects of using different control regimes and input conditions on the kinematics,
198 contact mechanics, and wear of the same TKR design. A computational model, that

199 has previously been validated for the same TKR design as that used in this study,
200 (Abdelgaied, Fisher and Jennings 2018) was used to investigate the kinematics,
201 contact mechanics and wear under all conditions investigated. Experimental
202 simulation was used to investigate the contact mechanics (contact area) under all
203 conditions investigated, and to determine wear using the Leeds gait displacement
204 control input conditions. In addition, experimental wear rates obtained under ISO-
205 14243-1 2009 force control standard, using the same TKR and same simulator
206 (Johnston, et al. 2018, Johnston, et al. 2019), were used to further validate the study.

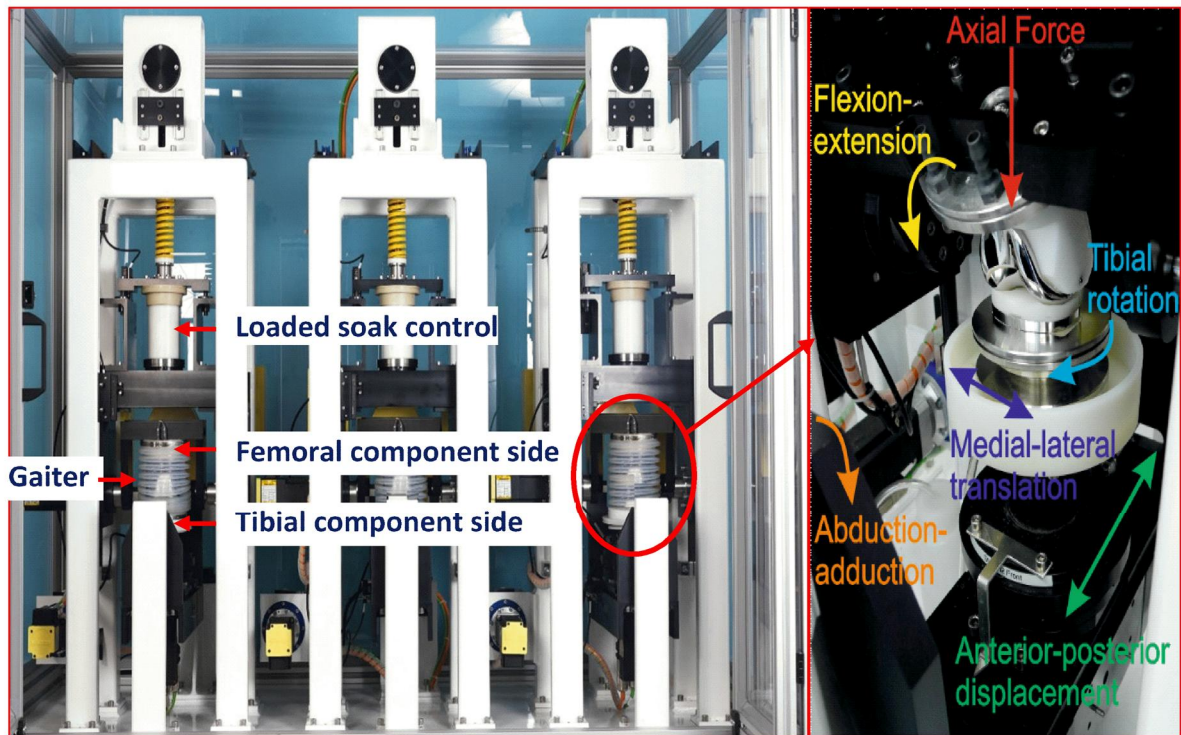
207

208 Mid-size (size 3) Sigma fixed bearing cruciate retaining total knee replacements
209 (DePuy Synthes, UK) comprising Co-Cr-Mo alloy femoral components, and polished
210 Co-Cr-Mo tibial trays, were used throughout with curved polyethylene tibial inserts.
211 The inserts were moderately cross-linked UHMWPE (XLK™) (GUR 1020, 5Mrad
212 gamma irradiation). In the experimental simulation studies, six sets of bearings were
213 mounted anatomically in each of the six simulator stations. For all test methods, the
214 central axis of each implant was offset from the aligned axes of applied load from the
215 centre of the joint by 7% of its width in the medial direction, in accordance with the
216 ISO recommendation (ISO-14243-1, 2009, ISO-14243-3, 2014). The centre of
217 rotation of the femoral components was taken as either an average centre of the
218 femoral distal and posterior radii, for ISO test methods, or as the distal radius of the
219 implant, as indicated by the device design, for Leeds gait.

220

221 Experimental simulation was run using a six station electromechanically driven knee
222 simulator (Simulation Solutions, UK). The simulator had six fully independent stations
223 in two banks; three stations per bank (Figure 1). Each station had six degrees of
224 freedom with five controlled axes of motion – axial force to the femoral component,
225 femoral flexion extension, tibial internal-external rotation, tibial anterior-posterior
226 displacement, and tibial adduction-abduction rotation (Abdelgaied, Fisher and
227 Jennings 2017).

228



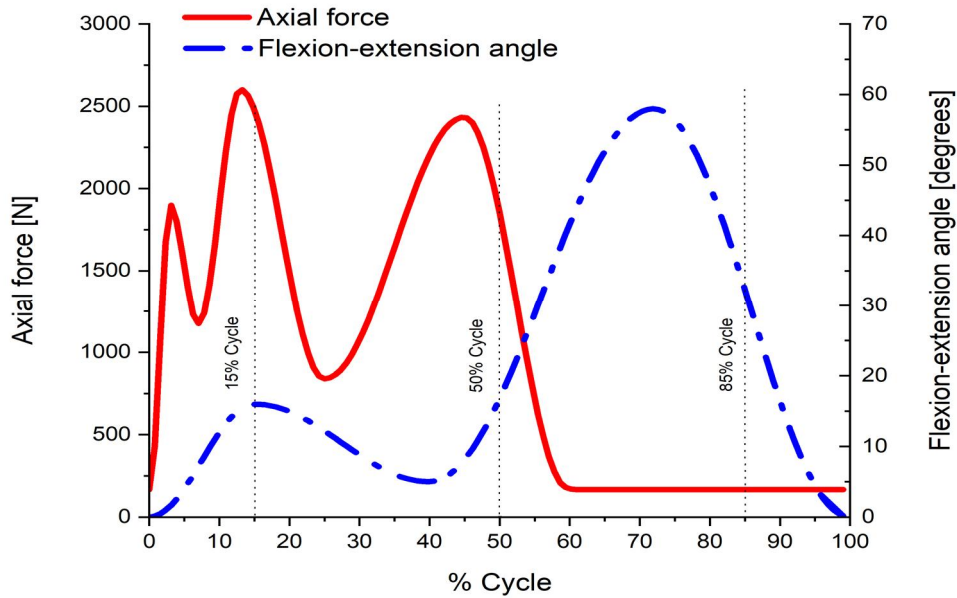
229
 230 Figure 1: Six station electromechanically driven knee simulator (Simulation Solutions,
 231 UK), and the six degrees of freedom for each station.

232
 233

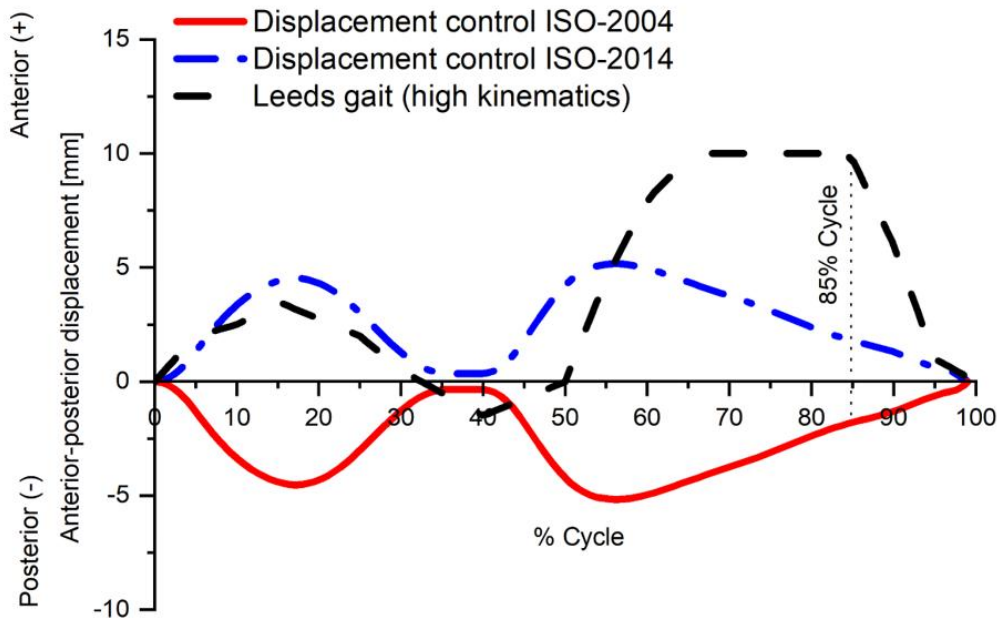
234 Two different test control methods were investigated; displacement control (ISO-
 235 14243-3-2004, ISO-14243-3-2014, and Leeds gait) and force control (ISO-14243-1-
 236 2009) test methods. Axial force and flexion-extension angle were common for all test
 237 methods (Figure 2.a). AP translation (Figure 2.b) and tibial rotation (Figure 2.c)
 238 motions were displacement controlled in ISO-14243-3-2004 and ISO-14243-3-2014,
 239 with the only difference being a reversal of AP displacement and tibial rotation
 240 polarities between the two standards. The test setup and soft tissue constraints were
 241 used in accordance with ISO recommendations (ISO-14243-1 2009, ISO-14243-3
 242 2014, ISO-14243-3 2004). In addition, the Leeds gait displacement controlled
 243 method, which includes axial force and flexion-extension as defined by the ISO
 244 standards, with AP displacement and tibial rotation motions based on the work by
 245 Lafortune et al. (Lafortune, et al. 1992) was also investigated (Figure 2). Six samples
 246 were studied for each condition.

247 For ISO-14243-1-2009 force control test method, AP translation and tibial rotation
 248 motions were force controlled (Figure 3). The test setup and soft tissue constraints

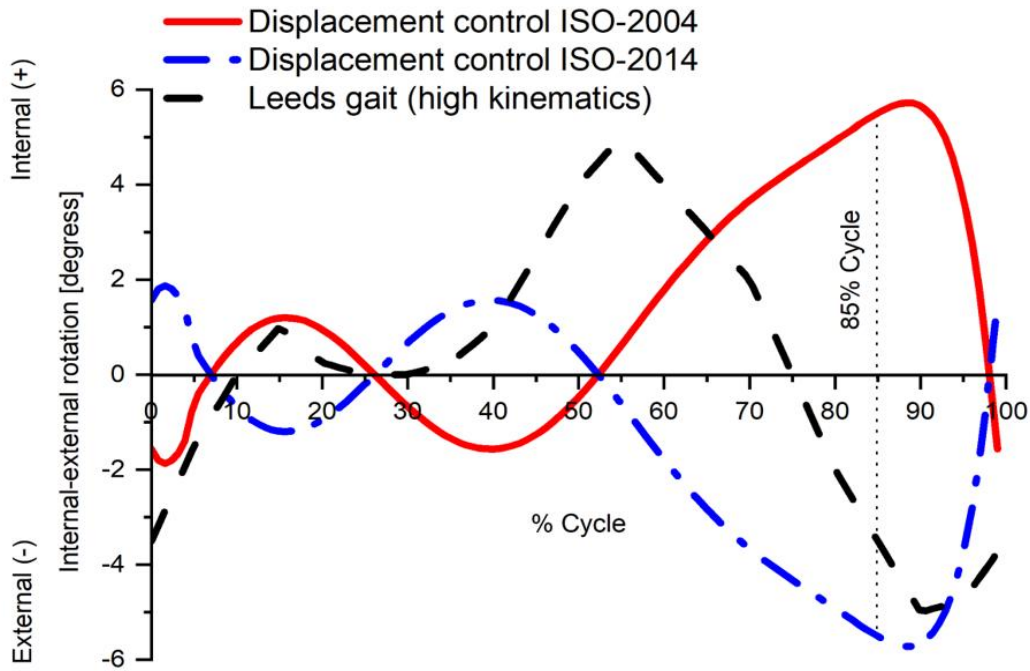
249 were used in accordance with ISO recommendations (ISO-14243-1 2009, ISO-14243-
 250 3 2014, ISO-14243-3 2004).
 251



252
 253 Figure 2.a: Axial force and flexion-extension angle input profiles for all test methods.
 254

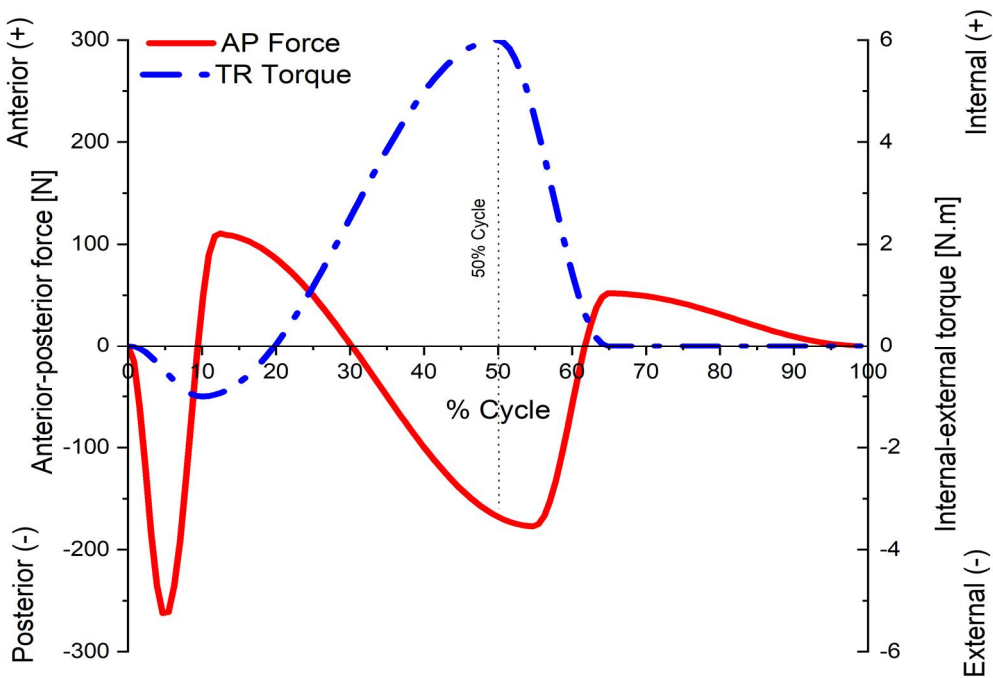


255
 256 Figure 2.b: Anterior-posterior displacement input profiles for different displacement
 257 controlled test methods (ISO-14243-3 2014, McEwen, et al. 2005, Barnett, et al.
 258 2001, ISO-14243-3 2004).
 259



260
261
262
263
264

Figure 2.c: Tibial rotation input profiles for different displacement controlled test methods (ISO-14243-3 2014, McEwen, et al. 2005, Barnett, et al. 2001, ISO-14243-3 2004).



265
266
267
268

Figure 3: Anterior-posterior force and internal-external tibial rotation torque input profiles for the ISO force controlled test method(ISO-14243-1 2009, ISO-14243-3 2014).

269

270 The total contact scar area on each tibial bearing insert was determined
271 experimentally for every input condition. This experimental contact mechanics
272 simulation was run for 1000 cycles, for each condition. An ink and Vaseline mixture
273 was spread between the articulating surfaces (Figure 3), and the removal of the ink
274 mixture reflected the total contact area. Photographs were taken from above each
275 tibial insert with a digital camera. Calibrated images were used to determine the total
276 contact scar areas using Image Pro software (Image Pro, v6.3, USA. The studies
277 were carried out on all six stations of the knee simulator using six independent
278 samples. 100 consecutive cycles (during the 1000 cycles test) of kinetics and
279 kinematics from a six axis load cell (on the tibial side) and anterior-posterior and tibial
280 rotation position sensors were recorded for each station. The average total contact
281 scar area, and output kinematics for the 100 cycles across all the stations was
282 calculated and presented with 95% confidence intervals (CI).

283

284 The experimental wear simulation was run for 3 million cycles of Leeds gait. The
285 simulator was run at a frequency of 1Hz. The lubricant used was new-born calf serum,
286 diluted to 25%, supplemented with 0.03% (v/v) sodium azide to retard bacterial growth,
287 and was changed every 0.33 million cycles. Prior to testing, all inserts were soaked in
288 deionised water for a minimum period of four weeks. This allowed an equilibrated fluid
289 absorption level to be achieved prior to the commencement of the wear study, reducing
290 variability due to fluid weight gain. Wear was determined gravimetrically at one million
291 cycle measurement intervals throughout the study. A Mettler XP205 (Mettler-Toledo,
292 USA) digital microbalance, which had a readability of 0.01mg, was used for weighing
293 the bearing inserts. The volumetric wear was calculated from the weight loss
294 measurements, using a density of 0.93 mg/mm³ for the polyethylene material, and
295 using unloaded soak controls to compensate for moisture uptake. The cumulative
296 volumetric wear was calculated for each station and the mean wear rate was then
297 calculated for all 6 stations (mean \pm 95% Confidence Intervals).

298

299 A validated computational simulation model was used to predict contact area, contact
300 stress, sliding distances, and wear, utilising elastic contact mechanics and a
301 modification of Archard's law where the wear volume is defined as a function of
302 contact area, sliding distance, cross-shear and non-dimensional contact stress

303 (Abdelgaied, Fisher and Jennings 2018). The model was used to run different test
304 methods investigated and, for the ISO force control method, was used to predict AP
305 displacement and tibial rotation angle. Each condition was simulated for 3 million
306 cycles, each cycle was split into 127 steps (the same number of steps as the
307 experimental simulator inputs), and the insert geometry was updated at 0.5 million
308 cycles to account for the surface changes due to surface wear (Abdelgaied et al.
309 2018). The computational model simulated the ProSim knee simulator and followed
310 the appropriate recommendations for each of the test methods investigated.
311 The tibial and the femoral components were meshed using quadratic tetrahedral
312 elements (C3D10M). An isotropic coefficient of friction of $\mu = 0.04$ was assumed in a
313 penalty contact formulation to describe the contact between the tibial and femoral
314 contact surfaces. Polyethylene was defined as an elastic material using equivalent
315 Poisson's ratio and elastic modulus of the XLK inserts. The input equivalent Poisson's
316 ratio and elastic modulus of the XLK inserts (GUR 1020, 5Mrad gamma irradiation),
317 were 0.32 and 553 MPa respectively (Abdelgaied, Fisher and Jennings 2018). These
318 parameters were determined from mechanical tests under compressive conditions
319 and accounted for the plastic deformation of polyethylene (Abdelgaied, Fisher and
320 Jennings 2018). The contact area, contact stress, and sliding distance predictions
321 from the computational simulation were recorded for each step during the simulation.
322 Where needed, the predictions at 15% (high axial force), 50% (high AP force and
323 tibial rotation torque), and 85% (high AP displacement, tibial rotation angle, and
324 flexion-extension angle) through the gait cycle, as shown in Figure 2, were presented.
325 Root-mean square error was calculated as a metric to quantify the difference in
326 computationally predicted and experimentally measured kinematics.
327 The data associated with this article are openly available through the University of
328 Leeds data repository (Abdelgaied & Jennings 2022).

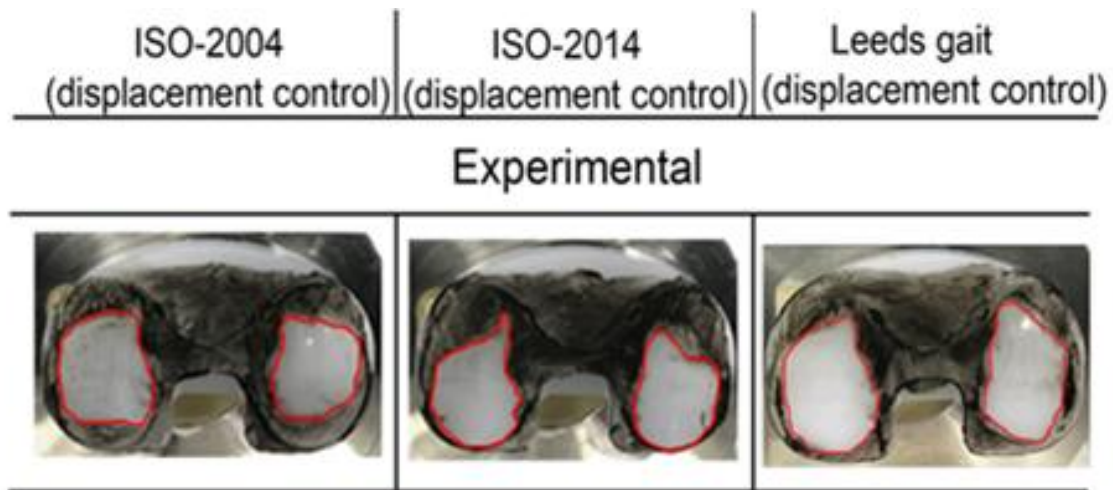
329

330 **Results:**

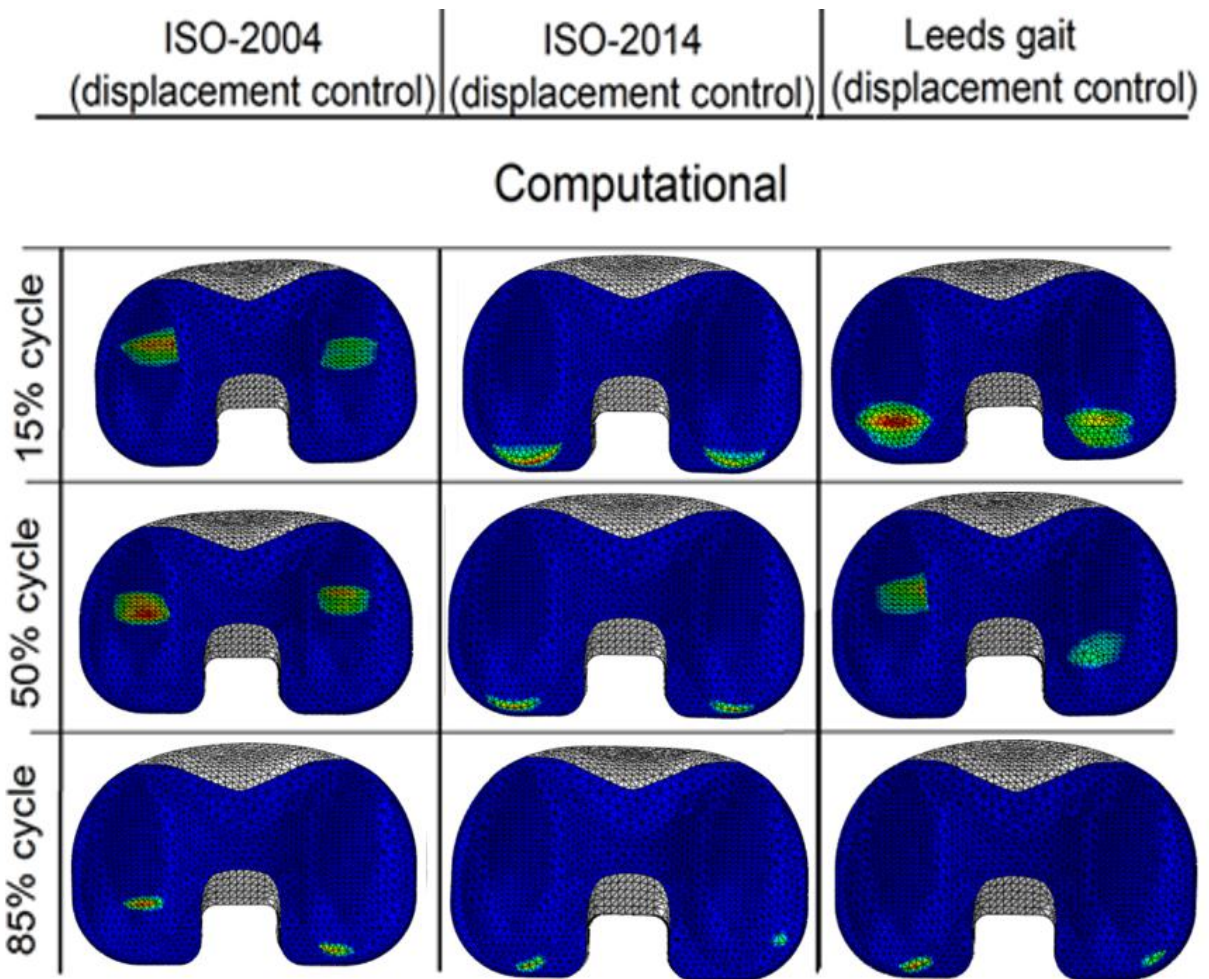
331 **Part One: Displacement control test methods:**

332 Experimental total contact scar examples of the Sigma TKR with XLK inserts, under
333 different displacement control test methods, are shown in Figure 4.a. The contact
334 area using the more recent displacement control ISO-14243-3-2014 inputs was
335 located more posteriorly compared to that using displacement control ISO-14243-3-
336 2004. The total contact scars using the displacement control Leeds gait were larger

337 and shifted posteriorly compared to that of the displacement control ISO-14243-3-
 338 2014 and ISO-14243-3-2004 profiles. The average total contact scar areas using the
 339 displacement control ISO-14243-3-2004, ISO-14243-3-2014, and Leeds gait profiles
 340 were 958 ± 39 , 876 ± 55 , and 1087 ± 63 [mm²] respectively (mean \pm 95% CI, n=6). The
 341 contact stresses, taken as an indication of contact scar areas, determined
 342 computationally at 15%, 50%, and 85% through the gait cycle, are shown in Figure
 343 4.b. In addition, the total contact areas determined computationally at different points
 344 through the gait cycle, for different test methods, are shown in Figure 4.c. The
 345 computationally predicted total contact area from ISO 2014 was generally lower than
 346 that predicted from ISO 2004 and Leeds gait test methods. In addition, the anterior-
 347 posterior displacement and tibial rotation angle of the lowest point of the medial
 348 condyle are shown in Figure 4.d and Figure 4.e respectively.



349
 350 Figure 4.a: Experimental total contact scar areas using different displacement control
 351 test methods
 352



353

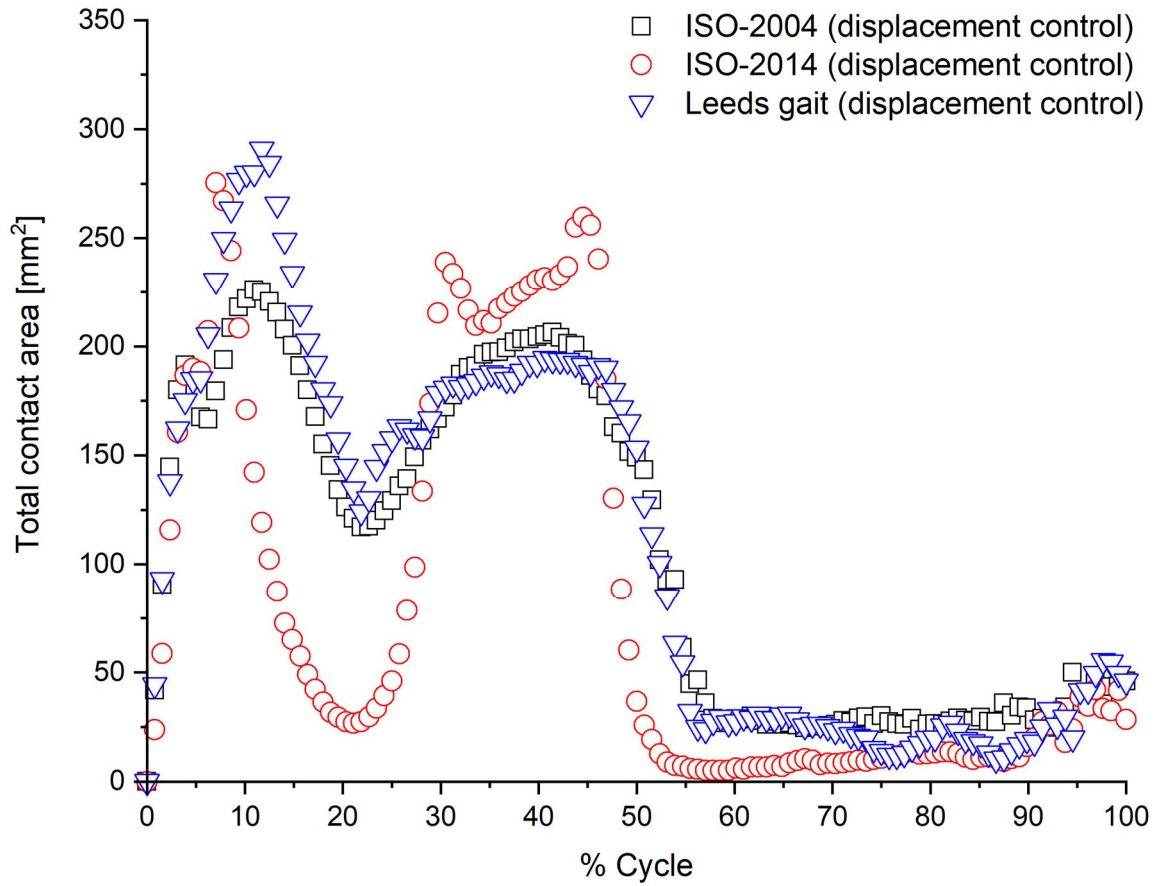
354 Figure 4.b: Computational contact scars at 15%, 50%, and 85% through the gait cycle

355 using different displacement control test methods (more points throughout the cycle

356 are openly available through the University of Leeds data repository (Abdelgaied &

357 Jennings 2022))

358



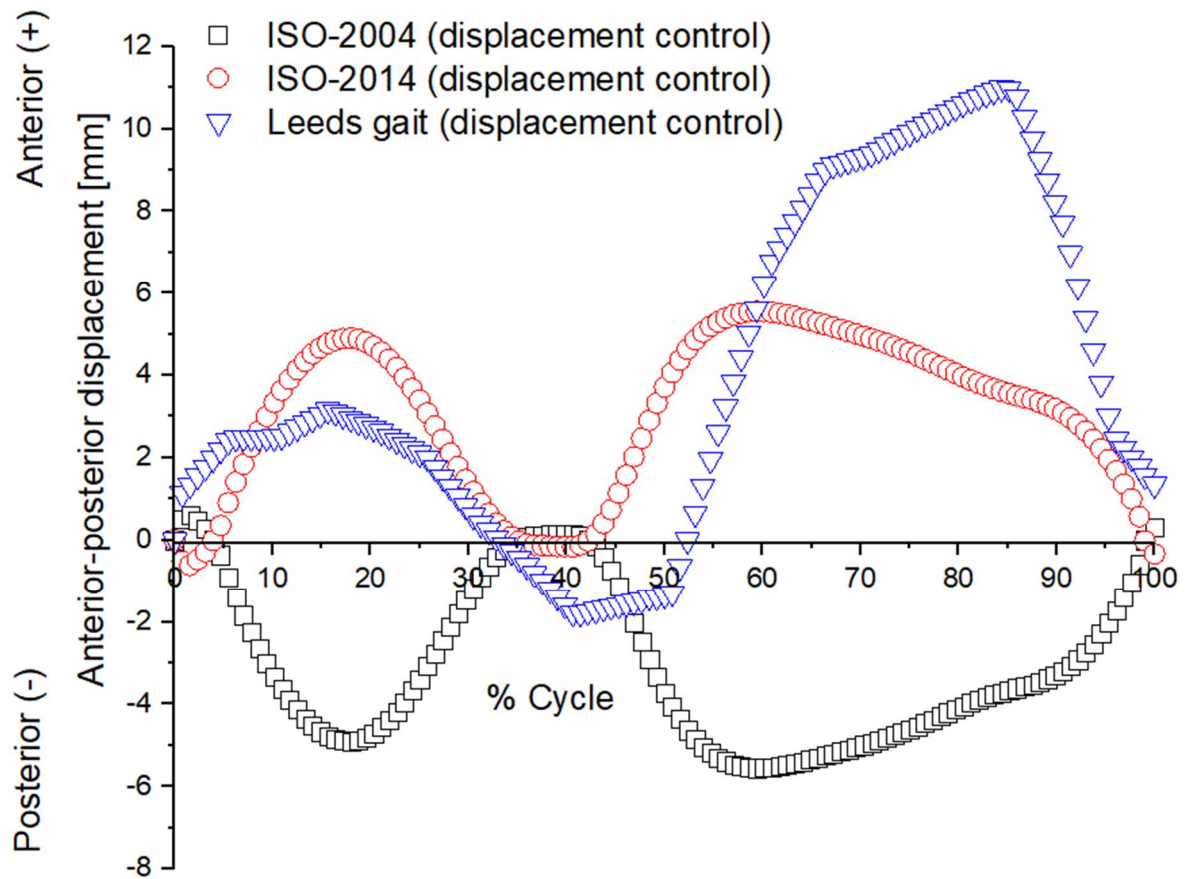
359

360 Figure 4.c: Computational total contact areas at different points through the gait cycle

361

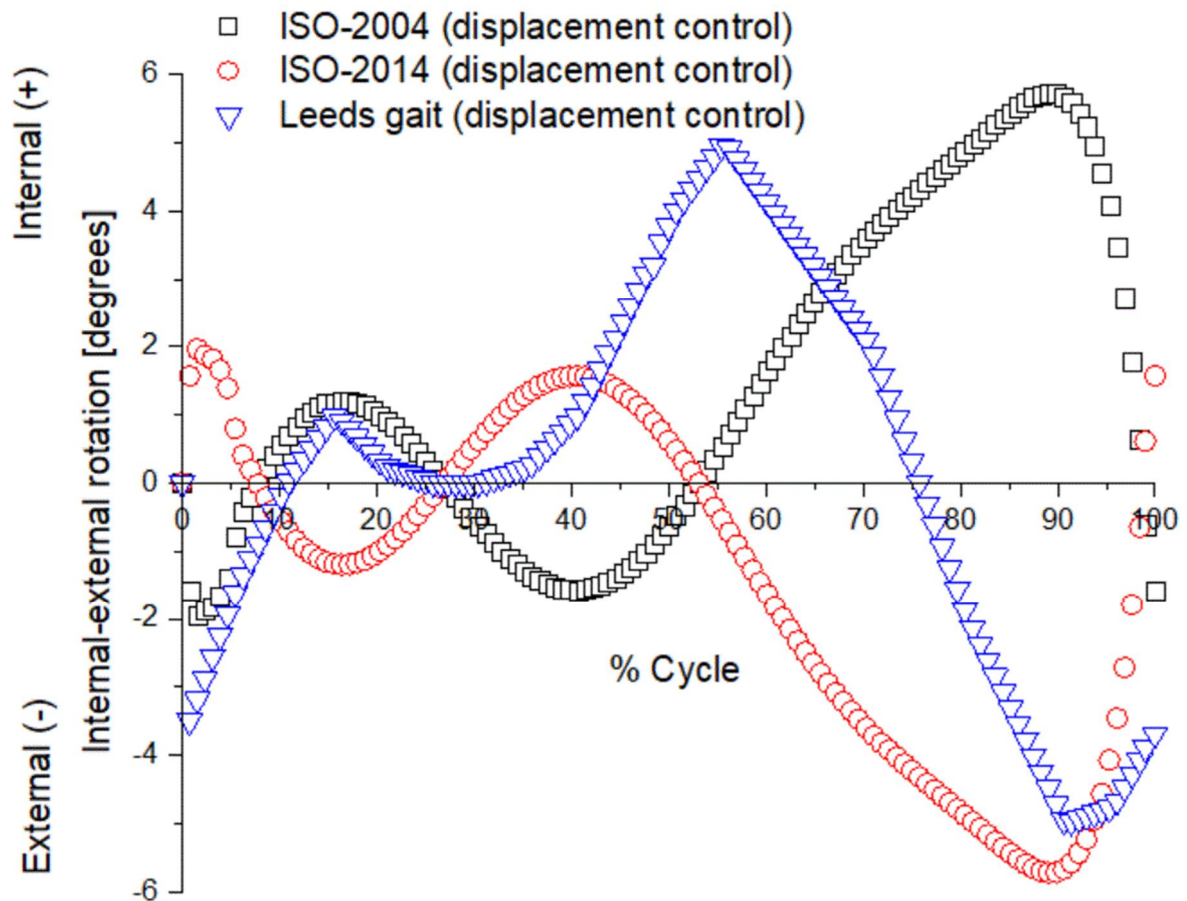
using different displacement control test methods

362



363

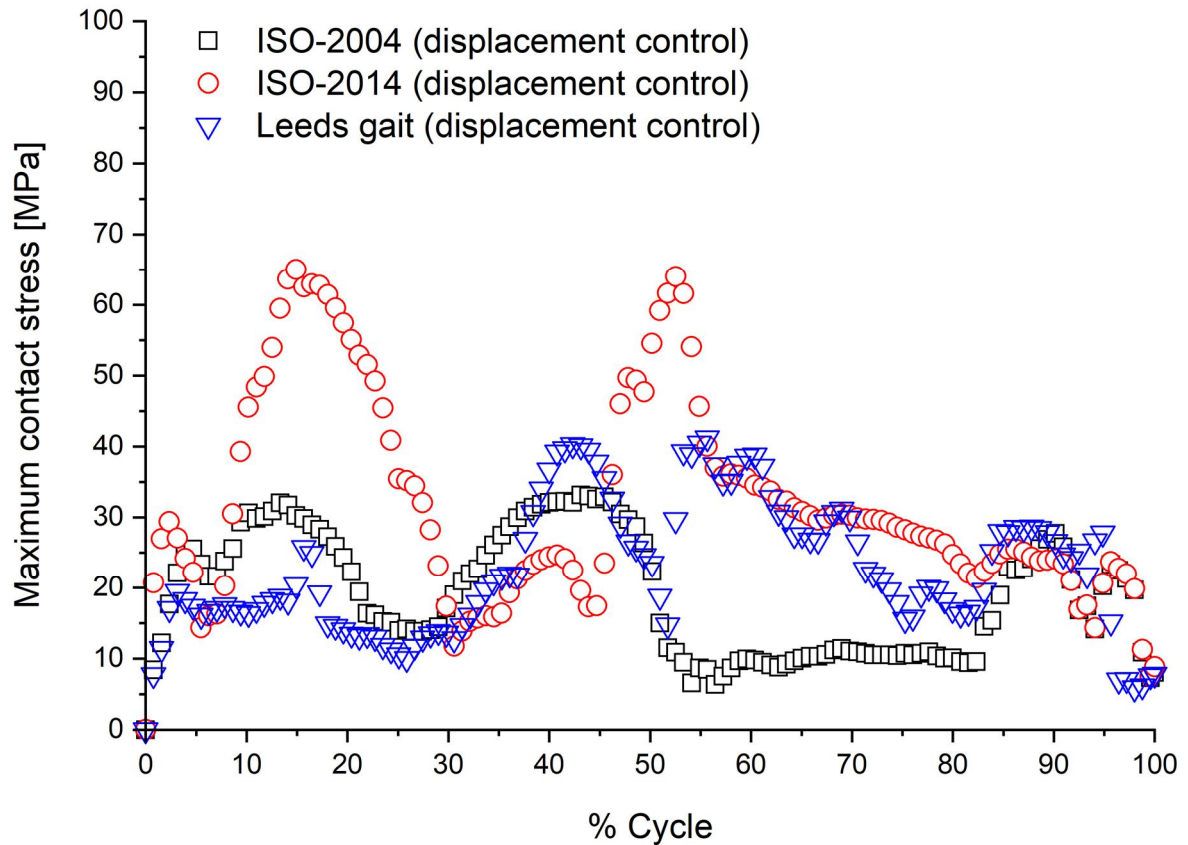
364 Figure 4.d: Computationally predicted anterior-posterior displacement [mm] of the
 365 lowest point of the medial condyle using different displacement control test methods
 366



367

368 Figure 4.e: Computationally predicted tibial rotation angle [degrees] of the lowest
 369 point of the medial condyle using different displacement control test methods
 370

371 The computationally predicted maximum contact stress at each step of the gait cycle
 372 is shown in Figure 5. For displacement control, reversing the AP displacement and
 373 tibial rotation directions in the displacement control ISO-2014, compared to ISO-2004,
 374 resulted in high contact stresses of more than 65 MPa, at the posterior edge of the
 375 inserts.



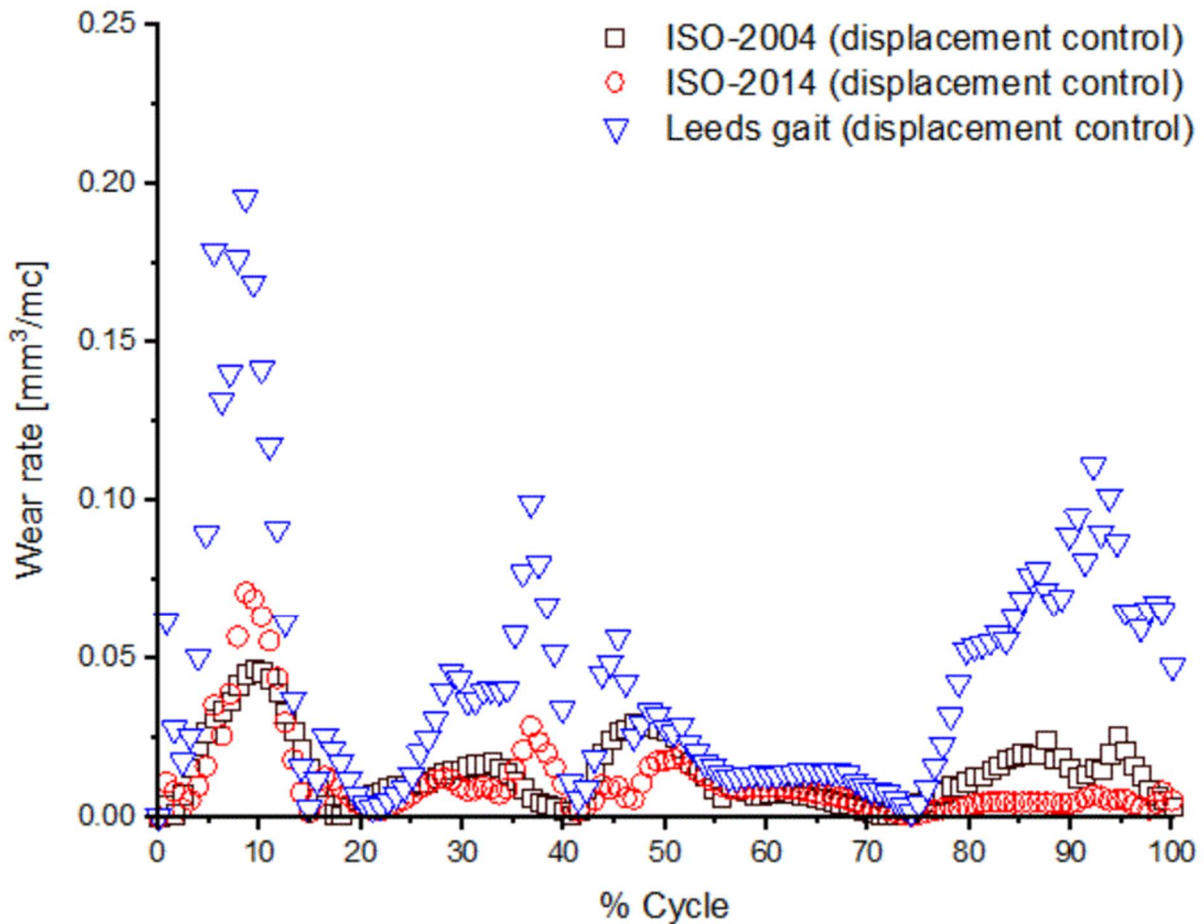
376

377 Figure 5: Computationally predicted maximum contact stress [MPa], at different
 378 percentages through the gait cycle, for different displacement control test methods.

379

380 The computationally predicted wear rates were 1.8, 1.4, and 5.6 [mm³/million cycles]
 381 for ISO-14243-3-2004, ISO-14243-3-2014, and Leeds gait respectively. The
 382 experimental wear rate for the Leeds gait condition was 5.02±2.1 mm³/million cycles
 383 (mean ± 95% CI, n=6). The computationally predicted wear rate [mm³/ million cycles],
 384 at different percentages through the gait cycle, for different displacement control test
 385 methods is shown in Figure 6.

386

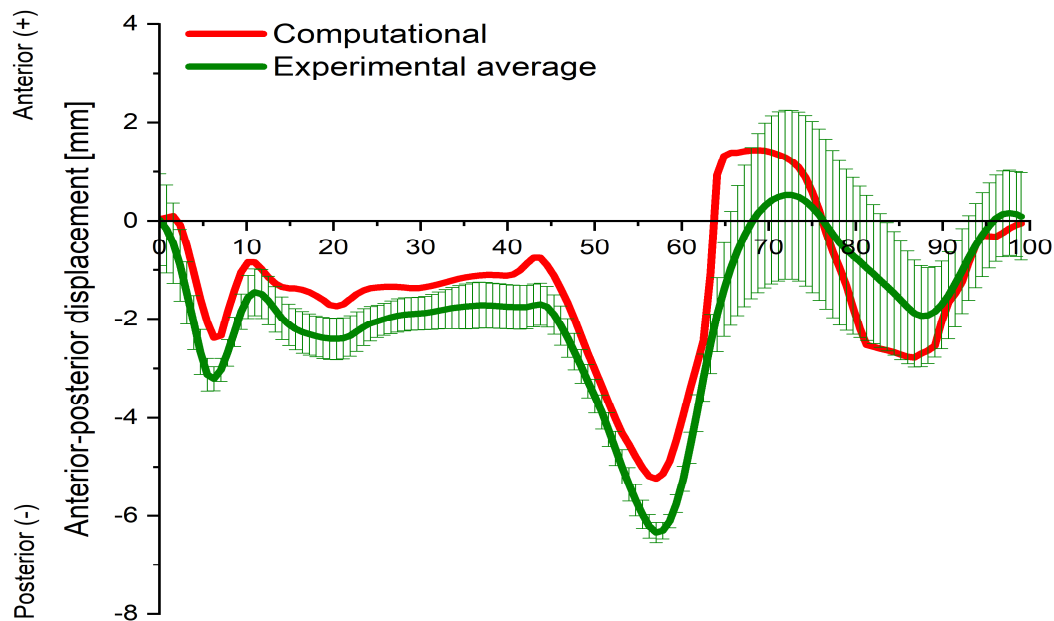


387
 388 Figure 6: Computationally predicted wear rate [$\text{mm}^3/\text{million cycles}$], at different
 389 percentages through the gait cycle, for different displacement control test methods.
 390

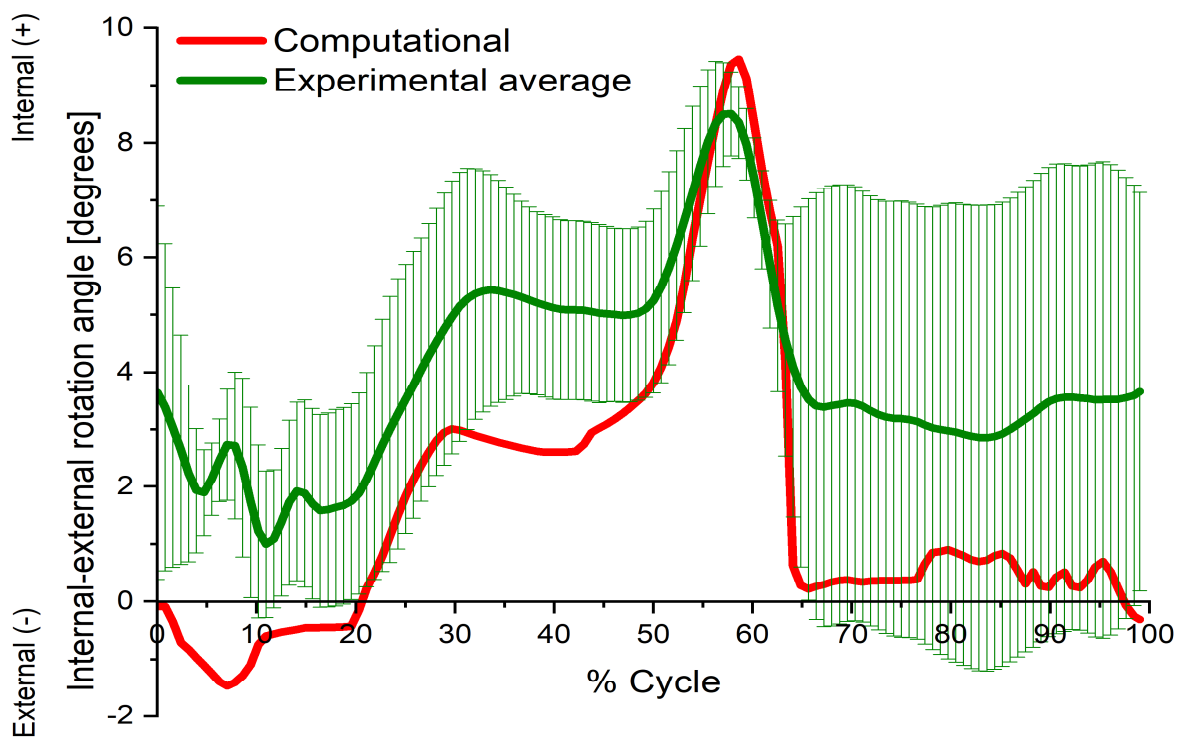
391 **Part Two: Force control test method:**

392 The computationally predicted AP displacement and tibial rotation angle using the
 393 force control ISO-2009 inputs are shown in Figure 7 and Figure 8 respectively
 394 alongside those obtained from the experimental simulation. The predicted AP
 395 displacement and tibial rotation angle ranged between -5.3 and 1.5 [mm] and
 396 between -1.4 and 9.5 [degrees] respectively. The predicted AP displacements were in
 397 generally good agreement with the measured average experimental values (root-
 398 mean square error ~ 0.9). The root-mean square error between the predicted tibial
 399 rotation angles and the measured average experimental values was approximately
 400 0.5. There was however a large variation in the measured experimental tibial rotation
 401 values and the predicted tibial rotation angles were mostly within the 95% CI of the
 402 experimental measurements. In addition, the anterior-posterior displacement and
 403 tibial rotation angle of the lowest point of the medial condyle are shown in Figure 9.

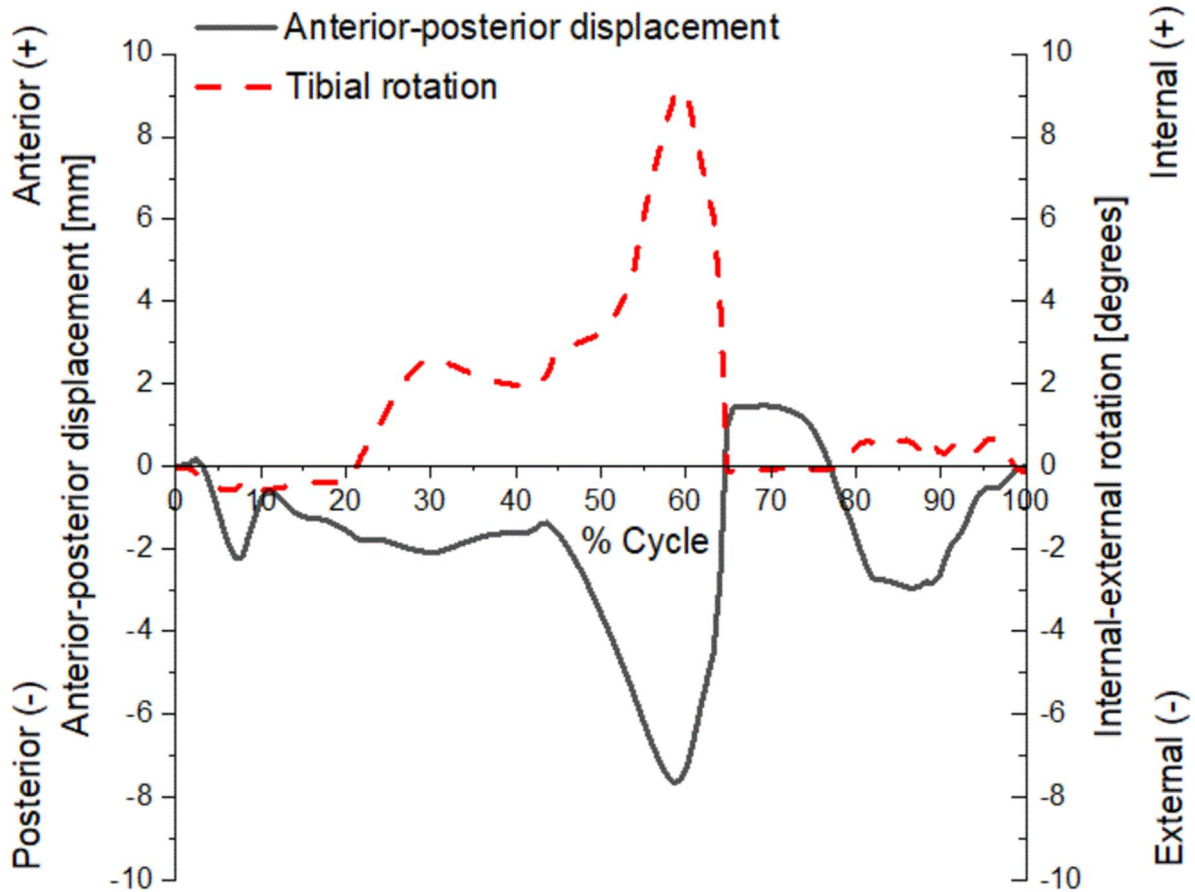
404



406 Figure 7: Computationally predicted AP displacements [mm] compared to
 407 experimental AP displacements [mm] (mean \pm 95% CI, n=100 cycles) using the force
 408 control ISO-2009 input kinematics.



409 Figure 8: Computationally predicted tibial rotation angle [degrees] compared to
 410 experimental tibial rotation angle [degrees] (mean \pm 95% CI, n=100 cycles) using the
 411 force control ISO-2009 input kinematics.



412

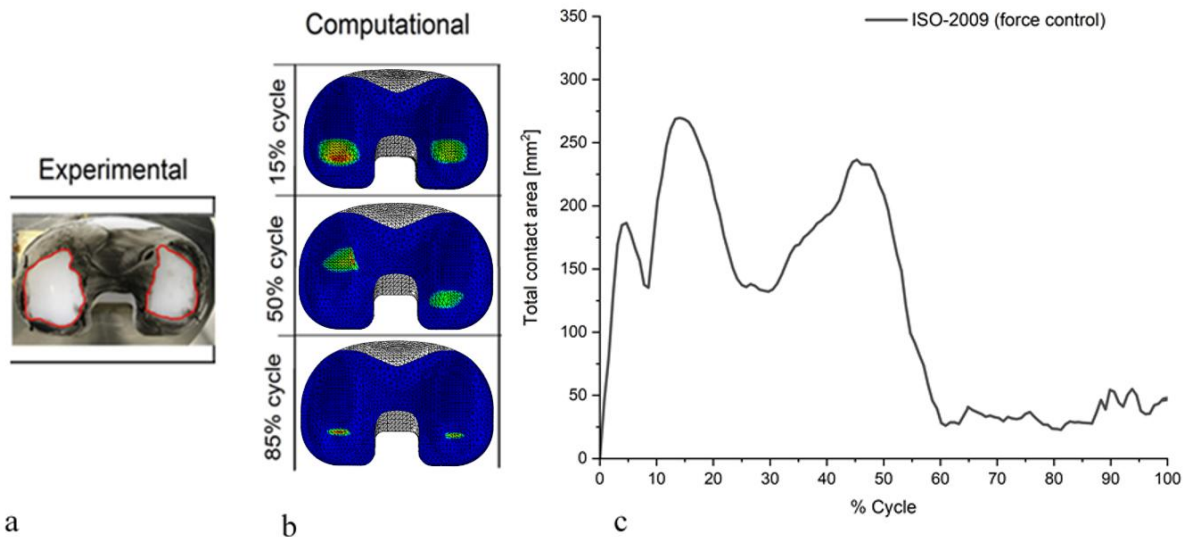
413 Figure 9: Computationally predicted anterior-posterior displacement [mm] and tibial
 414 rotation angle [degrees] of the lowest point of the medial condylar using ISO-14243-1-
 415 2009 force control test method

416

417 The experimental total contact scar areas of the Sigma TKR with XLK inserts using
 418 the force control ISO-14243-1-2009 are shown in Figure 10.a. The contact area scars
 419 using the force control ISO-14243-1-2009 were located more towards the centre of
 420 the inserts. The average total contact area using the force control ISO-14243-1-2009
 421 was 1031 ± 67 [mm²] (mean \pm 95% CI, n=6). The contact stresses, indicative of
 422 contact scars, determined computationally at 15%, 50%, and 85% through the gait
 423 cycle, are shown in Figure 10.b. In addition, the total contact areas determined
 424 computationally at different points through the gait cycle are shown in Figure 10.c.
 425 The computationally predicted total contact areas from ISO-14243-1-2009 and Leeds
 426 gait were generally similar.

427

428



429

a

b

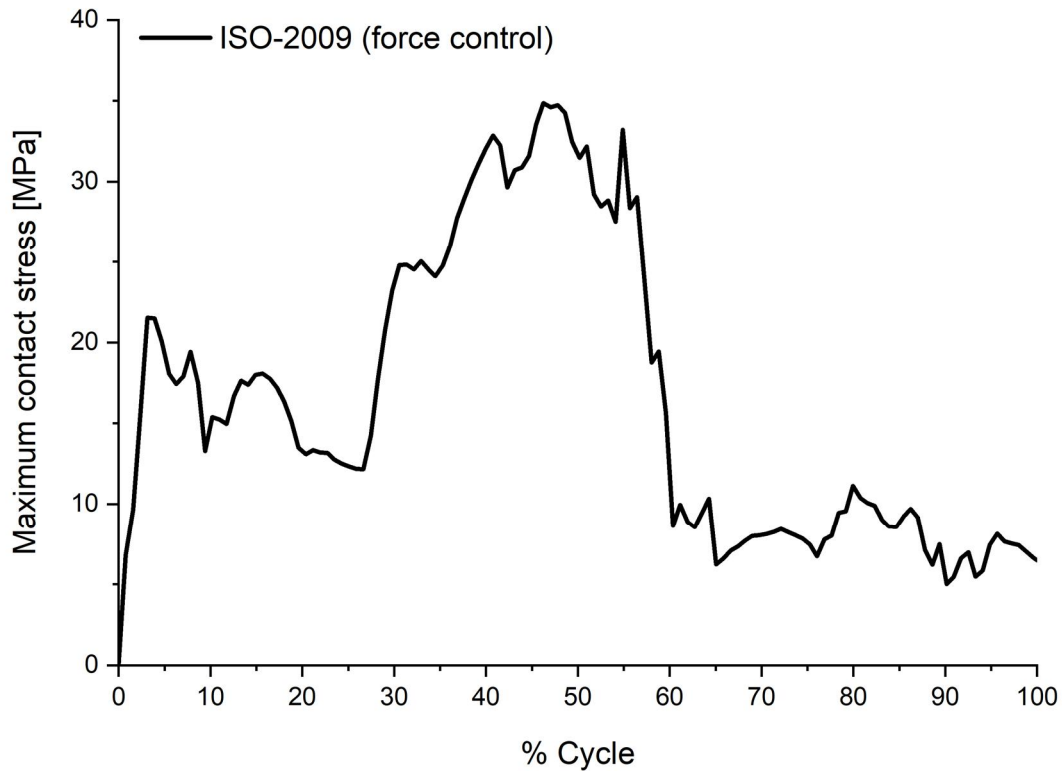
c

430 Figure 10: (a) Experimental total contact scars, (b) computational contact scars at
 431 15%, 50%, and 85% through the gait cycle, (c) computational total contact areas at
 432 different points through the gait cycle using ISO-14243-1-2009 force control test
 433 method

434

435

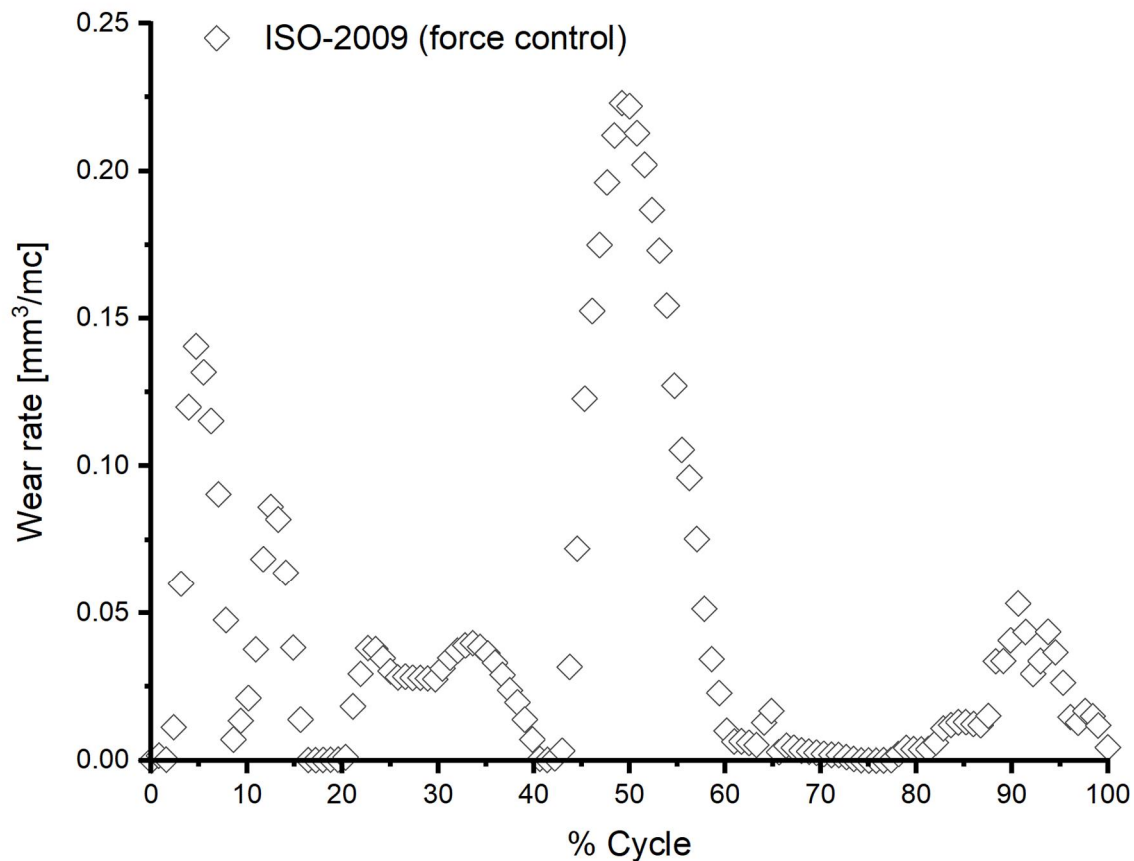
436 The computationally predicted maximum contact stress at each step of the gait cycle
 437 is shown in Figure 11. The predicted maximum contact stress though the gait cycle
 438 was approximately 35 MPa.



439
 440 Figure 11: Computationally predicted maximum contact stress [MPa], at different
 441 percentages through the gait cycle, for ISO-14243-1-2009 force control test method.

442
 443
 444 The computationally predicted wear rate for the force control ISO-14243-1-2009 was
 445 5.4 [mm³/million cycles]. The computationally predicted wear rate [mm³/ million
 446 cycles], at different percentages through the gait cycle is shown in Figure 12.

447



448

449 Figure 12: Computationally predicted wear rate [mm³/ million cycles], at different
 450 percentages through the gait cycle, for ISO-14243-1-2009 force control test method.

451

452 **Discussion:**

453 Different versions of standards and test methods to determine the wear of total knee
 454 replacements have adopted different approaches to control regimes, input profiles,
 455 centres of rotation, and polarity of motions. Each of these parameters affects the
 456 effective motions at the articulating surfaces of TKR and therefore, results in different
 457 contact mechanics, kinematics, and wear in TKR. The effects of using these different
 458 control regimes and input conditions on the contact mechanics, kinematics, and wear
 459 of any one TKR have not been fully investigated. The current study is the first study to
 460 investigate the kinematics, contact mechanics and wear performance of a TKR (a
 461 size 3 Sigma fixed bearing cruciate retaining total knee replacement, DePuy Synthes,
 462 UK) when running under ISO force and displacement control standards test
 463 conditions (ISO-14243-3-2004 displacement control, ISO-14243-3-2014 displacement
 464 control, and ISO-14243-1-2009 force control) as well as Leeds gait inputs (based on
 465 the work by (Lafortune, et al. 1992)), using experimental and computational

466 simulation methods. The study is a significant step towards understanding the
467 mechanical and tribological outcomes predicted by the different standard conditions in
468 order to choose a suitable test method for the preclinical evaluation of TKRs and to
469 make a better-informed choice of test conditions for different design solutions. This
470 will also help to understand differences in results from different test centres.

471

472 **Part One: Displacement Control test methods:**

473 Reversing AP displacement and tibial rotation angle profiles in the displacement
474 control standard ISO-2014, compared to the ISO-2004 standard, resulted in the
475 contact shifting more posteriorly, as shown from both experimental and computational
476 results in Figure 4. With ISO 2014 inputs, the AP motion of the tibial insert is
477 predominantly in the anterior direction (relative to the neutral position at the start of
478 the cycle), producing femoral rollback similar to Leeds gait and clinical data, with two
479 mean peaks of ~ 5 mm at ~15% and 55% of the cycle. However, reversing AP
480 displacement and tibial rotation angle profiles in the displacement control standard
481 ISO-2014, compared to the ISO-2004 standard, resulted in reduced contact areas
482 with high stress edge loading on the posterior lip of the insert, for this TKR design and
483 size, as shown in Figure 4 and Figure 5. The combined effect of decreased contact
484 area and increased contact stress seemed to dominate the wear prediction from the
485 computational model and resulted in a slight reduction in the computationally
486 predicted volumetric wear rate using ISO-2014, compared to ISO-2004, of
487 approximately 10%. It is recognised that the predicted volumetric wear rate also
488 depends on many factors, such as sliding distance and cross-shear, however, ISO-
489 2014 and ISO-2004 had the same AP displacement and tibial rotation profiles, but
490 with different polarities, and therefore similar sliding distances and cross-shear ratios
491 at the articulating surfaces.

492

493 Although Leeds gait kinematics produced femoral rollback, similar to the
494 displacement control standard ISO-2014 and clinical data, it did not result in high
495 stress edge loading on the posterior lip of the insert, as shown in Figure 4 and Figure
496 5. This can be attributed to both the different input kinematics, and different femoral
497 centre of rotation adopted in the Leeds gait test methods compared to the
498 displacement control standard ISO-2014. The distal centre of rotation of the femoral
499 component and input kinematics adopted in Leeds gait test methods, which aligns

500 more closely to the stance phase centre of rotation when loading is high, maintained
501 a more centred contact between femoral and the tibial components, with no edge
502 loading on the posterior lip of the insert, and resulted in a maximum contact stress of
503 approximately 40 MPa, compared to a maximum contact stress of more than 65 MPa
504 under the displacement control standard ISO-2014. In addition, the predicted wear
505 rate under the Leeds kinematic profiles was more than double that predicted under
506 the displacement control ISO-2004 and ISO-2014 standards due to the increased AP
507 and tibial rotation motion in the Leeds kinematics. Note that the Leeds gait test
508 method predates the displacement control ISO standard (Barnett, et al. 2001).

509

510 **Part Two: Force Control test methods:**

511 Force control test methods are relevant to fixed pivot bearing designs or highly
512 constrained bearings, where soft tissues are sacrificed or not present functionally. It
513 can also be used with other bearings provided that artificial ligament constraints are
514 used. When artificial ligament constraints are used with force control test methods,
515 these artificial soft tissue constraints control the motion kinematics, contact
516 mechanics, and therefore wear in non-highly constrained bearings. So, defining soft
517 tissue constraints defines the resultant kinematics, similar to defining input kinematics
518 in displacement control test methods.

519

520 The experimental and computational AP displacement of the tibial insert using ISO
521 2009 force control standard was mainly in the posterior direction (was only in the
522 anterior direction between ~63% and 76% of the cycle). The tibial rotation angle of
523 the tibial insert using ISO 2009 force control inputs, was ~ 2 degrees in the internal
524 direction at the start of the cycle, ranging between ~2 degrees in internal direction
525 and 2 degrees in the external direction for the first half of the cycle before reaching its
526 peak of ~6 degrees in the external direction at ~85% of the cycle. However, the
527 experimental and computational tibial rotation of the tibial insert using the ISO 2009
528 force control inputs was mainly in the internal direction (relative to the neutral position
529 of the insert to the femur at the start of the cycle). However, there was some variation
530 between the stations of the simulator under ISO-2009 force profiles, particularly
531 during the swing phase, when the low-tension (soft tissue) control springs were
532 applied. The high variation meant that comparison to the computational predictions
533 was less clear. This variation was partly attributed to station related factors, such as

534 friction between bearings, weight of the station, and the zero position at the start of
535 the test (Johnston, et al. 2018). This is a limitation of any force control method.

536

537

538 **General Discussion:**

539 The predicted total AP and tibial rotation displacement ranges from ISO-2009 were
540 ~25% and ~45% higher than the corresponding displacement inputs in ISO-2014,
541 respectively. This increase in motions could explain the increase in wear rate under
542 ISO-2009 compared to that under ISO-2014. In addition, the differences between the
543 resultant kinematics from the force control ISO-2009 and the input kinematics to the
544 displacement control ISO-2014 may also explain the differences in the contact
545 mechanics between the two test methods, shown in Figures 4, 5, 10, and 11. The
546 predicted total AP displacement from ISO-2009, of 6.8 mm (from -5.3 mm to 1.5 mm)
547 was almost a half of the Leeds kinematics displacement inputs (from -3.5 mm to 10
548 mm). However, the tibial rotation ranges were similar at 10.9 degrees and 10 degrees
549 from ISO-2009 and Leeds kinematics respectively. Although the average wear rates
550 from the force control ISO-2009, of 4.71 ± 1.29 mm³/million cycles (Johnston, et al.
551 2018), and Leeds gait, of 5.02 ± 2.1 [mm³/million cycles], were similar (< 7% difference
552 from both experimental and computational results), it should be noticed that the force
553 control ISO-2009 produced different kinematics compared to the Leeds kinematic
554 conditions. The predicted wear rates under the Leeds kinematic and the force control
555 ISO-2009 profiles were more than double that predicted under the displacement
556 control ISO-2004 and ISO-2014 standards due to the increased AP and tibial rotation
557 motion profiles in the Leeds kinematics and predicted from the ISO-2009 force control
558 standard compared to the displacement control ISO-2004 and ISO-2014 AP and tibial
559 rotation motion profiles (Figures 4, 6, 7, 8, 9 and 12).

560

561 Force control test methods are in effect just another different set of standard
562 conditions, where artificial soft tissue effectively defines actual kinematics simulated,
563 unless the design controls the displacement as in a medial pivot knee design.

564 However, the differences in kinematics, contact mechanics, and wear behaviour
565 between the ISO force and ISO displacement test methods, from both experimental
566 and computational results, imply that the two test methods are completely different
567 and therefore results from the two methods should be interpreted with caution. It

568 should be noted that a standard is a test method standard, not a performance
569 standard, and results from different standards cannot be compared. Therefore, results
570 from force control standard test methods should not be compared to results from any
571 of the displacement control standard test methods. In addition, results from any one
572 standard method need to be compared to a predicated device using an identical
573 standard test method.

574
575 Through dynamic videofluoroscopy measurements of 6 patients with a DePuy
576 unilateral PFC Sigma Curved cruciate retaining (CR) fixed-bearing TKA, Schutz et al.
577 (2019) measured the tibio-femoral kinematics throughout complete cycles of walking,
578 stair descent, sit-to-stand and stand-to-sit. Their study showed that the measured
579 kinematics were task dependant and subject specific. In comparison with this study,
580 the predicted kinematics under ISO force control ISO-14243-1-2009 from our study
581 showed similar trend and polarity for the output anterior-posterior displacement
582 profiles, and the ISO-14243-3-2014 displacement control profiles better reflected the
583 trend and polarity of tibial rotation. However, the kinematics from neither ISO-14243-
584 1-2009 force control nor ISO displacement control ISO-14243-3-2014 test methods
585 fully reflected the magnitude and polarity of the posterior anterior displacement and
586 tibial rotation profiles from the in vivo fluoroscopic measurements made on this similar
587 implant used in this study (Schutz, et al. 2019). However, these in vivo fluoroscopic
588 measurements were taken from a relatively small number of TKR recipients; it is
589 recognised TKRs operate under a wide set of conditions in the patient population and
590 a portfolio of standard preclinical conditions are needed to simulate the range of
591 performances seen in the patient population. While preclinical simulation should
592 always be undertaken in comparison to a device with proven clinical history, these
593 results indicate the choice of simulated test conditions, even for similar TKR designs
594 with similar material properties, result in different kinematics, contact mechanics, and
595 wear of the bearing materials and may well influence the outcome of such
596 comparisons. However, it should be emphasised that different test methods are
597 required and should be utilised to answer different research questions. Although ISO
598 2009 force control test method allows the joint to move according to the applied
599 forces, joint design, alignment of the joint, and the soft tissue constraints and account
600 for the effects of other factors, such as friction and deformation of the articulating
601 surfaces, on the performance of TKR, displacement control kinematics eliminate

602 these effects and allow studies to answer specific questions. However, the
603 differences between different test methods should be fully understood. In order to
604 develop displacement control inputs specific to a certain TKR design or size,
605 computational models could be used to predict displacements from the TKR
606 responses to the force control profiles. These computationally predicted kinematics
607 could then be used as displacement control inputs where required.

608

609 **Limitations:**

610 There are some limitations to the current study. Firstly, the experimental wear study
611 was conducted for Leeds gait (high) kinematics test method only. This was mainly
612 due the high cost and time required to run the experimental simulations. However, the
613 computational model, used to predict the wear rates where no experimental data was
614 available, has previously been validated under three different kinematic conditions
615 (Abdelgaied, Fisher and Jennings 2018). In addition, the predicted wear rate under
616 the force control ISO-2009 of $5.4 \text{ mm}^3/\text{million cycles}$ was within the 95% confidence
617 limits of the reported experimental wear rate for the same TKR, of 4.71 ± 1.29
618 $\text{mm}^3/\text{million cycles}$ (Johnston, et al. 2018), which gives confidence in the model.
619 Secondly, although the variation in the input tibial torque was within the ISO
620 recommended tolerances for all stations (ISO-14243-1-2009), there was some
621 variation between the stations of the simulator under ISO-2009 force profiles,
622 particularly during the swing phase, when the low-tension control springs were
623 applied. The high variation meant that comparison to the computational predictions
624 was less clear. This variation was partly attributed to station related factors, such as
625 friction between bearings, weight of the station, and the zero position at the start of
626 the test (Johnston, et al. 2018). This is a limitation of any force control method.
627 Finally, the results of the study are limited to the tested TKR design. Different TKR
628 designs could show different kinematic, contact mechanics, and wear behaviours
629 under different test protocols.

630

631 **Conclusion:**

632 This study showed differences in the kinematics, contact mechanics, and wear
633 between ISO 2009 force, ISO displacement (ISO 2004 & ISO 2014), and Leeds
634 kinematics test methods and between ISO displacement standards with different AP
635 displacement and tibial rotation polarities (ISO 2004 & ISO 2014) for a single

636 prosthesis design. Different standards are in fact different test methods, not
637 performance standards. No single standard can be considered correct or better than
638 another standard. Each standard must be used with its own predicate control results
639 from a device with clinical history and results across different standards should never
640 be compared. Clinically, the kinematics in the population are extremely variable,
641 which results in highly variable wear rates. While a standard method is necessary, on
642 its own it is not adequate and needs to be supported by tests under a portfolio of
643 representative conditions with different kinematic conditions, different soft tissue
644 constraints, as well as with different alignments, so that the variability and range of
645 wear rates expected clinically might be determined. This study enables further
646 progress towards the definition of such a portfolio of representative conditions, by
647 deepening the understanding of the relationships between currently used input
648 conditions and the resulting mechanical and wear outputs.

649
650

651 **Acknowledgments:**

652 This research work was supported by EPSRC, Innovate UK and BBSRC [IKC Medical
653 Technologies, EP/I019103/1], the Leeds Centre of Excellence in Medical Engineering
654 [WELMEC, funded by the Wellcome Trust and EPSRC, WT088908/Z/09/Z], the
655 EPSRC Centre for Innovative Manufacturing in Medical Devices [EP/K029592/1] and
656 the Leeds Musculoskeletal Biomedical Research Unit (LMBRU), funded by NIHR. JF
657 has been supported in part by the National Institute for Health Research (NIHR)
658 Leeds Biomedical Research Centre. The views expressed are those of the author(s)
659 and not necessarily those of the NHS, the NIHR or the Department of Health. JF has
660 been supported in part by EPSRC UKRI. This research work was supported by
661 DePuy Synthes, UK, who also supplied the components. The simulators were
662 developed and manufactured by Simulation Solutions, UK. The authors thank Phillip
663 Wood and the rest of the Institute of Medical & Biological Engineering technical team
664 for laboratory research support and assistance in this work.

665
666

667 **References:**

668 Abdelgaied, A., et al., 2014. The effect of insert conformity and material on total knee
669 replacement wear. *Proceedings of the Institution of Mechanical Engineers.Part H,*
670 *Journal of Engineering in Medicine*, 228 (1), 98-106.

- 671 Abdelgaied, A., Fisher, J. and Jennings, L.M., 2018. A comprehensive combined
672 experimental and computational framework for pre-clinical wear simulation of total
673 knee replacements. *Journal of the Mechanical Behavior of Biomedical Materials*, 78,
674 282-291.
- 675 Abdelgaied, A., Fisher, J. and Jennings, L.M., 2017. A comparison between
676 electromechanical and pneumatic-controlled knee simulators for the investigation of
677 wear of total knee replacements. *Proceedings of the Institution of Mechanical
678 Engineers.Part H, Journal of Engineering in Medicine*, 231 (7), 643-651.
- 679 Abdelgaied, A., et al., 2011. Computational wear prediction of artificial knee joints
680 based on a new wear law and formulation. *Journal of Biomechanics*, 44 (6), 1108-
681 1116.
- 682 Abdelgaied, A & Jennings LM, 2022. Data associated with " Understanding the
683 Differences in Wear Testing Method Standards for Total Knee Replacement".
684 [Dataset] <https://doi.org/...>(to be confirmed following review)
- 685 Asano, T., et al., 2007. Dose effects of cross-linking polyethylene for total knee
686 arthroplasty on wear performance and mechanical properties. *Journal of Biomedical
687 Materials Research.Part B, Applied Biomaterials*, 83 (2), 615-622.
- 688 Barnett, P.I., et al., 2001. Comparison of wear in a total knee replacement under
689 different kinematic conditions. *Journal of Materials Science.Materials in Medicine*, 12
690 (10-12), 1039-1042.
- 691 Brockett, C.L., et al., 2016. The influence of simulator input conditions on the wear of
692 total knee replacements: An experimental and computational study. *Proceedings of
693 the Institution of Mechanical Engineers.Part H, Journal of Engineering in Medicine*,
694 230 (5), 429-439.
- 695 Fisher, J., et al., 2010. 2009 Knee Society Presidential Guest Lecture: Polyethylene
696 wear in total knees. *Clinical Orthopaedics and Related Research*, 468 (1), 12-18.
- 697 Galvin, A.L., et al., 2009. Effect of conformity and contact stress on wear in fixed-
698 bearing total knee prostheses. *Journal of Biomechanics*, 42 (12), 1898-1902.
- 699 ISO-14243-1, 2009. Implants for surgery—wear of total knee joint prostheses. Part 1:
700 Loading and displacement parameters for wear testing machines with load control
701 and corresponding environmental conditions for test.
- 702 ISO-14243-1, 2002. Implants for surgery - Wear of total knee-joint prostheses - Part
703 1: Loading and displacement parameters for wear-testing machines with load control
704 and corresponding environmental conditions for test.
- 705 ISO-14243-3, 2014. Implants for surgery. Wear of total knee-joint prostheses.
706 Loading and displacement parameters for wear-testing machines with displacement
707 control and corresponding environmental conditions for test. British Standards
708 Institute.

709 ISO-14243-3, 2004. Implants for surgery. Wear of total knee-joint prostheses.
710 Loading and displacement parameters for wear-testing machines with displacement
711 control and corresponding environmental conditions for test. British Standards
712 Institute.

713 Jennings, L.M., et al., 2007. The influence of femoral condylar lift-off on the wear of
714 artificial knee joints. *Proceedings of the Institution of Mechanical Engineers.Part H,*
715 *Journal of Engineering in Medicine*, 221 (3), 305-314.

716 Johnson, T.S., Andriacchi, T.P. and Laurent, M.P., 2000. Development of a knee
717 wear method based on prosthetic in vivo slip velocity. *In:* pp. 46, 30.

718 Johnston, H., et al., 2019. The effect of surgical alignment and soft tissue conditions
719 on the kinematics and wear of a fixed bearing total knee replacement. *Journal of the*
720 *Mechanical Behavior of Biomedical Materials*, 100, 103386.

721 Johnston, H., et al., 2018. Representing the effect of variation in soft tissue
722 constraints in experimental simulation of total knee replacements. *Journal of the*
723 *Mechanical Behavior of Biomedical Materials*, 87, 87-94.

724 Lafortune, M.A., et al., 1992. Three-dimensional kinematics of the human knee during
725 walking. *Journal of Biomechanics*, 25 (4), 347-357.

726 McEwen, H.M., et al., 2005. The influence of design, materials and kinematics on the
727 in vitro wear of total knee replacements. *Journal of Biomechanics*, 38 (2), 357-365.

728 Morrison, J.B., 1970. The mechanics of the knee joint in relation to normal walking.
729 *Journal of Biomechanics*, 3 (1), 51-61.

730 National Joint Registry, 2020. 17th Annual Report.

731 National Joint Registry, 2014. *11th Annual Report*.

732 Paul, J.P., 1976. Force actions transmitted by joints in the human body. *Proceedings*
733 *of the Royal Society of London.Series B, Biological Sciences*, 192 (1107), 163-172.

734 Paul, J.P., 1970. The effect of walking speed on the force actions transmitted at the
735 hip and knee joints. *Proceedings of the Royal Society of Medicine*, 63 (2), 200-202.

736 Paul, J.P. and McGrouther, D.A., 1975. Forces transmitted at the hip and knee joint of
737 normal and disabled persons during a range of activities. *Acta Orthopaedica Belgica*,
738 41 Suppl 1 (1), 78-88.

739 Sathasivam, S. and Walker, P.S., 1997. A computer model with surface friction for the
740 prediction of total knee kinematics. *Journal of Biomechanics*, 30 (2), 177-184.

741 Sutton, L.G., et al., 2010. In vitro response of the natural cadaver knee to the loading
742 profiles specified in a standard for knee implant wear testing. *Journal of*
743 *Biomechanics*, 43 (11), 2203-2207.

744 Schutz, P., et al. Knee implant kinematics are task-dependent. J R Soc Interface.
745 2019;16(151):20180678. doi:10.1098/rsif.2018.0678

746 Walker, P.S., et al., 1997. A knee simulating machine for performance evaluation of
747 total knee replacements. *Journal of Biomechanics*, 30 (1), 83-89.

748

749

750

751